Soil Biology & Biochemistry 43 (2011) 126–132

Contents lists available at ScienceDirect

Soil Biology & Biochemistry

journal homepage: www.elsevier.com/locate/soilbio

Probing carbon flux patterns through soil microbial metabolic networks using parallel position-specific tracer labeling

Paul Dijkstra [a,*], Joseph C. Blankinship [a,1], Paul C. Selmants [b], Stephen C. Hart [c], George W. Koch [a,d], Egbert Schwartz [a], Bruce A. Hungate [a,d]

[a] Department of Biological Sciences, Northern Arizona University, P.O. Box 5640, Flagstaff, AZ 86011, USA
[b] Environmental Studies Department, University of California, Santa Cruz, CA 95064, USA
[c] School of Natural Sciences and Sierra Nevada Institute, University of California, Merced, CA 953434, USA
[d] Merriam Powell Center for Environmental Research, Northern Arizona University, Flagstaff, AZ 86011, USA

ARTICLE INFO

Article history:
Received 30 May 2010
Received in revised form
16 September 2010
Accepted 19 September 2010
Available online 28 October 2010

Keywords:
Stable isotopes
Carbon
C and N availability
Soil microbial biomass
C metabolism

ABSTRACT

In order to study controls on metabolic processes in soils, we determined the dynamics of $^{13}CO_2$ production from two position-specific ^{13}C-labeled pyruvate isotopologues in the presence and absence of glucose, succinate, pine, and legume leaf litter, and under anaerobic conditions. We also compared $^{13}CO_2$ production in soils along a semiarid substrate age gradient in Arizona. We observed that the C from the carboxyl group (C_1) of pyruvate was lost as CO_2 much faster than its other C atoms ($C_{2,3}$). Addition of glucose, pine and legume leaf litter reduced the ratio between $^{13}CO_2$ production from 1-^{13}C pyruvate and 2,3-^{13}C pyruvate ($C_1/C_{2,3}$ ratio), whereas anaerobic conditions increased this ratio. Young volcanic soils exhibited a lower $C_1/C_{2,3}$ ratio than older volcanic soils. We interpret a low $C_1/C_{2,3}$ ratio as an indication of increased Krebs cycle activity in response to carbon inputs, while the higher ratio implies a reduced Krebs cycle activity in response to anaerobic conditions. Succinate, a gluconeogenic substrate, reduced $^{13}CO_2$ production from pyruvate to near zero, likely reflecting increased carbohydrate biosynthesis from Krebs cycle intermediates. The difference in $^{13}CO_2$ production rate from pyruvate isotopologues disappeared 4–5 days after pyruvate addition, indicating that C positions were scrambled by ongoing soil microbial transformations. This work demonstrates that metabolic tracers such as pyruvate can be used to determine qualitative aspects of C flux patterns through metabolic pathways of soil microbial communities. Understanding the controls over metabolic processes in soil may improve our understanding of soil C cycling processes.

1. Introduction

Carbon (C) stored as soil organic matter represents the largest C pool in the terrestrial biosphere (Schlesinger and Andrews, 2000), and small changes of fluxes into and out of this pool may influence the atmospheric CO_2 concentration and interact with ongoing climate change. Current efforts to understand the mechanistic drivers of soil C cycling, microbial turnover, and soil organic matter stabilization are hampered by our inability to determine details of microbial physiology in soils. It is often postulated that soil microbial activity is C or nitrogen (N) limited (Allen and Schlesinger, 2004; Dijkstra et al., 2006; Vitousek and Howarth, 1991), but we can only test this physiological condition with relatively long-term nutrient additions (e.g. Allen and Schlesinger, 2004; Hobbie and Vitousek, 2000), the response to which may not only reflect the current condition but include indirect effects, such as changes in microbial community composition. Here, we introduce a new stable isotope technique to determine C fluxes through microbial metabolic networks. We postulate that understanding how C is processed through whole-community metabolism may provide new insights into the roles of microorganisms in element cycling and storage. This stable isotope technique is adapted from metabolic flux analysis used for microorganisms (Bago et al., 1999; Holms, 1996; Kiefer et al., 2004), plants (Kruger and Ratcliffe, 2009; Priault et al., 2009) and animals (Koletzko et al., 1998; Vo et al., 2004), and consists of adding small amounts of position-specific ^{13}C-labeled metabolic tracer isotopologue pairs to soil in parallel incubations, and determining $^{13}CO_2$ production as a function of their C-atom position.

* Corresponding author. Tel.: +1 928 523 0432; fax: +1 928 523 7500.
E-mail address: paul.dijkstra@nau.edu (P. Dijkstra).
[1] Current address: School of Natural Sciences and Sierra Nevada Research Institute, University of California, Merced, CA 953434, USA.

0038-0717/$ – see front matter © 2010 Elsevier Ltd. All rights reserved.
doi:10.1016/j.soilbio.2010.09.022

Pyruvate is an ideal metabolic tracer as it occupies a central place in the cell's metabolic network (Sauer and Eikmanns, 2005; Fig. 1). Carbon in position 1 of pyruvate (carboxyl-C) is predominantly released as CO_2 by pyruvate dehydrogenase, and may enter the Krebs cycle via anaplerotic reactions (via pyruvate carboxylase). Carbon in positions 2 and 3 is released in the Krebs cycle. Changes in the ratio of CO_2 fluxes produced from 1-^{13}C and 2,3-^{13}C-labeled pyruvate ($C_1/C_{2,3}$ ratio) should therefore reflect an altered flux through these pathways. Previous studies have used position-specific ^{13}C-labeled compounds to study C turnover and sorption in soil (Fisher and Kuzyakov, 2010; Haider and Martin, 1981; Kuzyakov, 1997; Näsholm et al., 2001).

We tested whether position-specific ^{13}C-labeled pyruvate used as a metabolic tracer could detect changes in metabolic flux patterns of soil microbial communities in response to substrate manipulation (glucose, succinate, pine and legume leaf litter), O_2 concentration, and as a function of soil substrate age. We hypothesized that high C availability (glucose and litter addition, soil with high C:N ratio) would increase relative Krebs cycle activity, and low O_2 concentrations would decrease it. Furthermore, we hypothesized that addition of succinate would decrease the $^{13}CO_2$ production from pyruvate because of an increased C flux from Krebs cycle to carbohydrate biosynthesis (gluconeogenesis).

2. Materials and methods

2.1. Glucose and succinate addition

Soil (0–10 cm depth, A-horizon; Typic Haplustoll) was collected from cold desert grassland near Flagstaff, AZ, USA (1760 m above sea level) on September 12, 2009. The area was dominated by C_4 grasses *Bouteloua eriopoda* and *Hilaria jamesii*. The climate was semiarid with a mean annual temperature of 12 °C, and 230 mm mean annual precipitation. Gravimetric soil moisture content was 3.1% (s.e. 0.01; $n = 4$). Soil δ^{13}C signature was −16.1‰ (s.e. 0.1, $n = 8$), while soil C content was 1.3% (s.e. 0.1) and soil N content was 0.12% (s.e. 0.01).

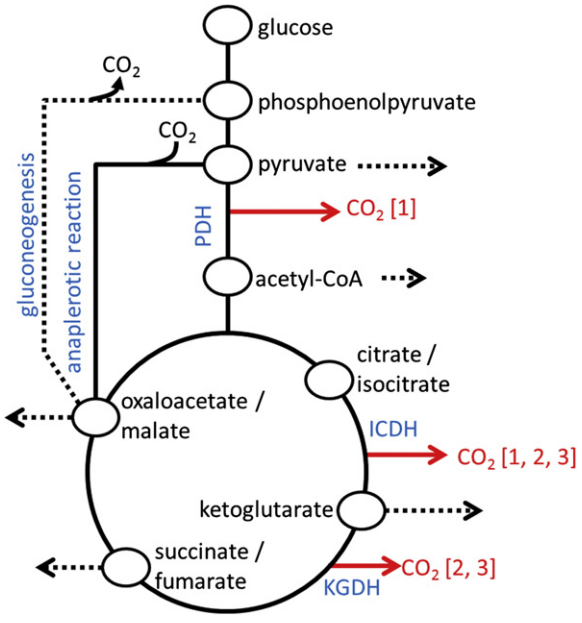

Fig. 1. Simplified model of metabolic processes in soil microbial cells assuming a glycolytic substrate. Solid arrows (red) indicate C transformations that release CO_2 from the pyruvate tracer (numbers in brackets indicate C-position of pyruvate lost as CO_2). Broken arrows indicate biosynthesis. Gluconeogenesis is normally suppressed when glucose is present. (For the interpretation of the reference to color in this figure legend the reader is referred to the web version of this article.)

Soil was sieved (2 mm mesh), air-dried and kept in the dark until used. Glucose (D-glucose, δ^{13}C −10.4‰, 10 mg per g soil) or succinate (δ^{13}C −25.1‰, 9.8 mg per g soil) was mixed with 50 g of soil. Control soil was similarly disturbed, but no substrate was added. Soil moisture content was increased to 21.5% (field capacity determined at −33 kPa according to Haubensak et al. (2002)). The soil was placed inside airtight Mason jars ($n = 4$; 473 ml volume; Jarden Company, Rye, NY, USA) and kept overnight in the dark.

Eighteen hours after incubation started, 10 ml of pure CO_2 (δ^{13}C −6.8‰) was added to the headspace and isotope composition of CO_2 in each jar was determined after 30 min. The injection of pure CO_2 was carried out to satisfy the instrument's requirement for a CO_2 concentration between 300 and 2000 μmol mol^{-1} and a gas supply rate of 20 ml min^{-1}. The production of $^{13}CO_2$ from pyruvate was calculated from the ^{13}C content of CO_2 in the ^{13}C-labeled incubation corrected for ^{13}C content of CO_2 from control soil. Jars were not opened between measurements.

Metabolic tracers were added 60 min later, as follows: two ml of a 3.2 mmol L^{-1} position-specific ^{13}C-enriched sodium pyruvate solution was added to the surface of the soil (0.13 μmol pyruvate per g soil) injected through a septum. Sodium pyruvate (Cambridge Isotope Laboratories, Andover, Massachusetts, USA) was either 99 at% ^{13}C-enriched in position 1 (C_1 – carboxyl group) or 99 at% ^{13}C-enriched in position 2 and 3 ($C_{2,3}$).

Isotope composition and concentration of CO_2 were determined before and 10, 20, 40, 60, 120 and 240 min after pyruvate addition. At each time, 10 ml of headspace air was injected into a Tedlar air-sample bag (Zefon International, Ocala, Florida) and diluted by CO_2-free air. The isotope composition of CO_2 was measured on a Picarro G1101-*i* CO_2 cavity ring-down isotope spectroscope (Picarro Inc., Sunnyvale, California, USA).

Soil respiration rates were determined over 24 h on parallel incubations. CO_2 concentration in the headspace was determined with a LICOR 6262. Headspace samples were injected into a 1-ml injection loop, and then flushed by a constant flow of N_2 gas into the measuring cell. CO_2 standards were used to correlate LICOR output to CO_2 concentrations. Data were analyzed using ANOVA with isotopologue as main effect and time as the repeated measure.

2.2. Effect of O_2 concentration

Soil (0–10 cm depth, A-horizon, Mollic Eutroboralf) was collected from a meadow in a ponderosa pine forest on September 21, 2009. Soil moisture at the time of sampling was 2.1% (s.e. 0.02, $n = 3$). Soil δ^{13}C signature was −21.9‰ (s.e. 0.2, $n = 7$), while % soil C and N concentration were 1.5% (s.e. 0.1) and 0.11% (s.e. 0.01) respectively. The soil was air-dried, and kept in the dark until used four days later. Water was added to bring soil to field capacity (27.3%). Anaerobic conditions were created by flushing the headspace with 100% N_2 gas. Control soils were incubated with ambient air. Soils were incubated overnight ($n = 4$). Eighteen hours after start of the incubation, 10 ml of pure CO_2 was added to the headspace. Measurement of CO_2 concentration and isotope composition started 30 min later, and 1-^{13}C and 2,3-^{13}C pyruvate was added 60 min after that. Isotope composition and concentration of CO_2 were determined before and 20, 40, 60 and 120 min after pyruvate addition (0.13 μmol per g soil).

2.3. Effect of litter addition

Soil from desert grassland was incubated (as described above) and mixed with ponderosa pine needles (10 mg g^{-1} soil; *Pinus ponderosa*, δ^{13}C −26.1; %N 1.0, C:N ratio 49.4) or legume leaves

(10 mg g^{-1} soil; *Lupinus argenteus* $\delta^{13}C$ −27.8‰, %N = 3.7, C:N ratio 12.1). Green leaves from lupine and needles from ponderosa pine were collected on 1 July 2009, dried at 60 °C overnight, ground to a fine powder, and stored at room temperature. Just before incubation, soil moisture content was adjusted to field capacity. After 18 h, 10 ml of pure CO_2 was added. Isotope composition and concentration of CO_2 were determined 10 min before and 20 and 60 min after adding 1-^{13}C and 2,3-^{13}C pyruvate (0.13 μmol per g soil). Soil respiration rate was determined over 24 h on parallel incubations.

2.4. Soils along a semiarid substrate age gradient

Soil was collected from intercanopy spaces in piñon-juniper woodlands (September 15, 2009; 0–10 cm depth, A-horizon) across a semiarid substrate age gradient (Substrate Age Gradient of Arizona; Selmants and Hart, 2008). Soils developed from similar volcanic deposits. Intercanopy spaces were dominated by *Bouteloua gracilis*, except for the youngest site where only a few C_3 shrubs were present. Substrate age was between 930 and 3,000,000 years (Table 1, Coyle et al., 2009; Selmants and Hart, 2008). Soils were sieved, air-dried, and incubated at field capacity for three days before 1-^{13}C and 2,3-^{13}C pyruvate was added (0.13 μmol per g soil, $n = 4$). Isotope composition and concentration of CO_2 were determined before and 20, 60, 120 and 240 min after adding pyruvate. Soil respiration rate was determined over 24 h on parallel incubations.

2.5. Long-term dynamics of pyruvate degradation

Soil from desert grassland (described above) was incubated for 22 days. 1-^{13}C and 2,3-^{13}C pyruvate was added at the start of the experiment. We sampled headspace CO_2 2 h, and 1, 2, 3, 7, 12, 15, 19, 22 d after pyruvate addition. For the first three days, 10 ml of pure CO_2 was injected into the headspace before the measurement; for the remaining days, enough CO_2 accumulated in the headspace so that no CO_2 addition was required. Headspace atmosphere was replaced by opening Mason jars for 30 min and flushing with lab air between measurements. Soil respiration rates were determined over 24 h on parallel incubations.

3. Results

3.1. Glucose and succinate addition

Total respiration rate increased in the presence of glucose and succinate (9.07 ± s.e. 0.68, 7.98 ± 0.71, and 0.92 ± 0.09 μg CO_2 g^{-1} soil h^{-1} for glucose-, succinate-amended and control soil respectively). The addition of glucose and succinate decreased the rate of $^{13}CO_2$ production from position-specific ^{13}C-labeled pyruvate. The $^{13}CO_2$ concentration increased approximately linearly between 0 and 120 min after pyruvate addition (Fig. 2; R^2 values between 0.99 for glucose-amended and 0.80 for succinate-amended soil). Significantly more $^{13}CO_2$ was produced from C_1 than $C_{2,3}$ (Fig. 2A, B). Rates of $^{13}CO_2$ production from 1-^{13}C pyruvate differed significantly from that from 2,3-^{13}C pyruvate (estimated from linear regression; Fig. 3) for the control and glucose-amended soil, but not significantly for the succinate addition. The ratio between the $^{13}CO_2$ production rates from the two isotopologues ($C_1/C_{2,3}$ ratio) declined with time (Fig. 3B) and was higher for control than glucose-amended soil ($P < 0.01$). The $C_1/C_{2,3}$ ratio for the succinate treatment was initially (not-significantly) lower, increased but then ended up at a similar value as for glucose-amended soil.

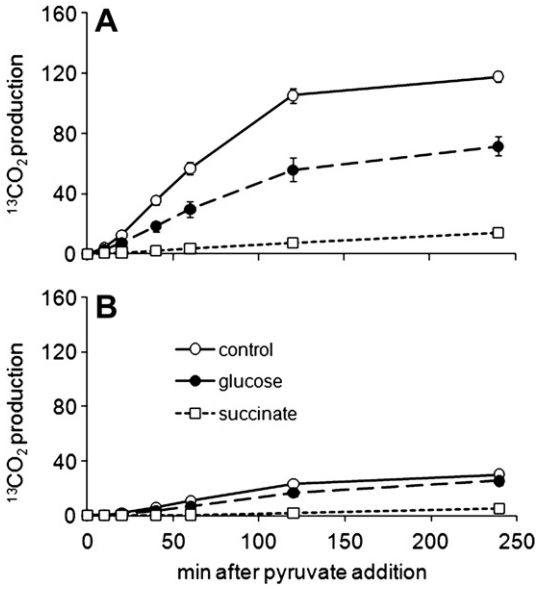

Fig. 2. Accumulated $^{13}CO_2$ production (nmol $^{13}CO_2$ g^{-1} soil) from 1-^{13}C (A) and 2,3-^{13}C (B) pyruvate against time since tracer addition (min). Soil incubated with and without glucose or succinate. Means and s.e.; $n = 4$. Interaction between treatment and time was significant ($P < 0.001$) for both pyruvate isotopologues (ANOVA with time as repeated measures).

3.2. Aerobic versus anaerobic conditions

The $^{13}CO_2$ release from 1-^{13}C pyruvate significantly exceeded that from 2,3-^{13}C pyruvate (Fig. 4) for aerobic soil, but not significantly for anaerobic soil during the first 60 min. The $C_1/C_{2,3}$ ratio was significantly higher for the anaerobic treatment (Fig. 4B).

3.3. Litter addition

Respiration rate increased after litter addition (control soil 0.6 ± 0.04; legume-amended soil 13.1 ± 0.18; pine-amended soil 7.5 ± 0.19 μg CO_2–C g^{-1} soil d^{-1}). As was observed after glucose addition, $^{13}CO_2$ production from 1-^{13}C and 2,3-^{13}C pyruvate

Table 1
Characteristics of soils and mean annual temperature (MAT, °C) and precipitation (MAP, mm) along the Substrate Age Gradient of Arizona.

Site	Soil type	Age (years)[a]	MAT/MAP (°C/mm)[a]	Soil C (mg g^{-1})[b]	Soil N (mg g^{-1})[b]	Micr. C[c] (μg g^{-1})[b]	$\delta^{13}C$ (‰)[b]	Clay (mg g^{-1})[a]	FC (%)[d]
Sunset Crater	Typic Ustorthent	930	12/328	8.0	0.44	29.5	−23.6	18	9
O' Neill Crater	Typic Durustand	55,000	11/352	13.7	1.27	113.9	−16.2	80	25
Red Mountain	Typic Argiustoll	750,000	11/325	26.6	2.14	259.7	−18.4	318	32
Cedar Mountain	Typic Haplustalf	3,000,000	11/333	13.7	1.24	148.4	−18.3	440	39

[a] Selmants and Hart (2008).
[b] Coyle et al. (2009).
[c] Micr. microbial.
[d] FC = field capacity determined according to Haubensak et al. (2002).

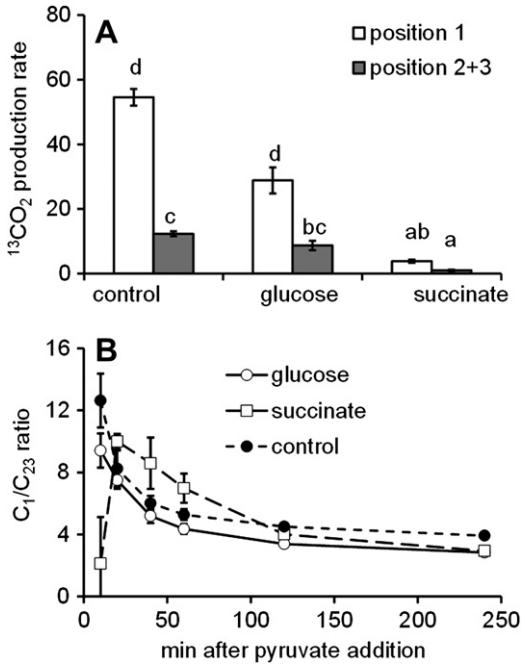

Fig. 3. $^{13}CO_2$ production rate (nmol $^{13}CO_2$ g^{-1} h^{-1}) from 1-^{13}C and 2,3-^{13}C pyruvate estimated from linear regression between 0 and 120 min after pyruvate addition (A) and instantaneous $C_1/C_{2,3}$ ratio against time (min, B) with and without glucose and succinate. Interaction between substrate and ^{13}C-position was significant ($P < 0.001$). Letters indicate significant differences (multiple means least-significant-difference test when ANOVA indicated significance).

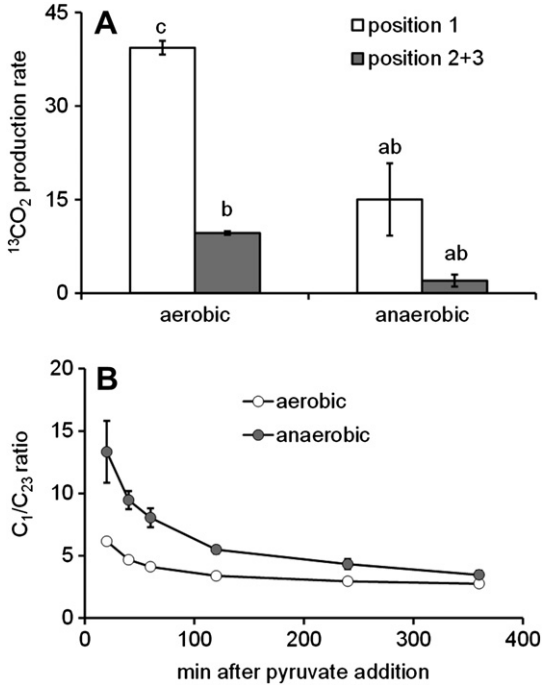

Fig. 4. $^{13}CO_2$ production rate (nmol $^{13}CO_2$ g^{-1} h^{-1}) from 1-^{13}C and 2,3-^{13}C pyruvate estimated from linear regression between 0 and 60 min after pyruvate addition (A) and instantaneous $C_1/C_{2,3}$ ratio against time (min; B) under aerobic and anaerobic conditions. Interaction between treatment and C-position was significant ($P < 0.01$). Letters indicate significant differences (multiple means least-significant-difference test when ANOVA indicated significance).

decreased in the presence of litter during the first 120 min (Fig. 5A). The $C_1/C_{2,3}$ ratio was significantly higher for pine than legume litter, and both were significantly reduced relative to the control (Fig. 5B).

3.4. Soils along a substrate age gradient

Soil substrate age significantly affected the rate of $^{13}CO_2$ production from 1-^{13}C and 2,3-^{13}C-labeled pyruvate and the $C_1/C_{2,3}$ ratio (Fig. 6). There were positive associations ($R^2 > 0.9$, $P < 0.1$) between the $C_1/C_{2,3}$ ratio and various measures of N cycling (soil total N, net N mineralization and gross nitrification; data not shown).

3.5. Longer-term $^{13}CO_2$ kinetics from the pyruvate tracer

Over the course of the incubation, total respiration rate declined (Fig. 7A). Such decline is often observed after soil disturbance (e.g. Hart et al., 1994). After 22 days, 93% of ^{13}C label from 1-^{13}C pyruvate was recovered, but only 37% of ^{13}C from 2,3-^{13}C pyruvate. The $^{13}CO_2$ production rate from pyruvate declined with time in two distinct phases. Initially, there were significant differences between the two isotopologues of pyruvate, but these differences disappeared during the second phase when the $^{13}CO_2$ production rates from both isotopologues exhibited a similar exponential decline (Fig. 7B).

4. Discussion

4.1. CO_2 production from pyruvate tracer

The carboxyl group from pyruvate was quickly lost as CO_2 (74% within 2 h after pyruvate addition, 91% after three days, and 93% after 22 days). In contrast, C in position 2 and 3 was retained and either incorporated into biomass or secreted from cells, and only 37% was released as CO_2 at the end of the 22-d incubation. This is not surprising as most microbial products that contain C_1 from

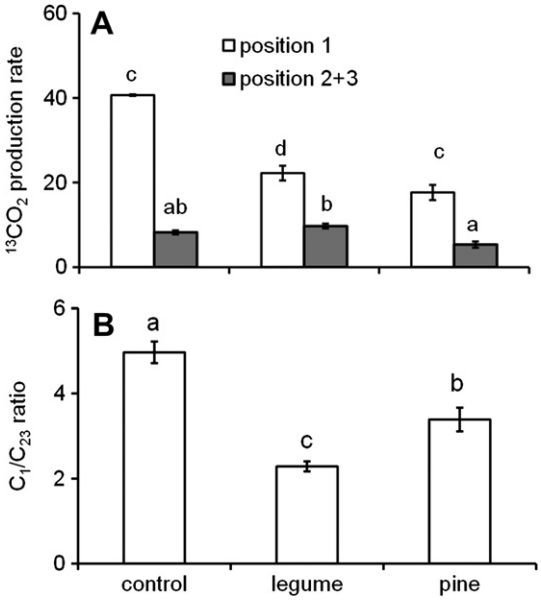

Fig. 5. $^{13}CO_2$ production rate from 1-^{13}C and 2,3-^{13}C pyruvate estimated from linear regression between 0 and 60 min after pyruvate addition (A) and $C_1/C_{2,3}$ ratio (B) for a control soil, and soil amended with legume and pine green leaf material. Interaction between treatment and C-position was significant ($P < 0.001$). Letters indicate significant differences (multiple means least-significant-difference test when ANOVA indicated significance).

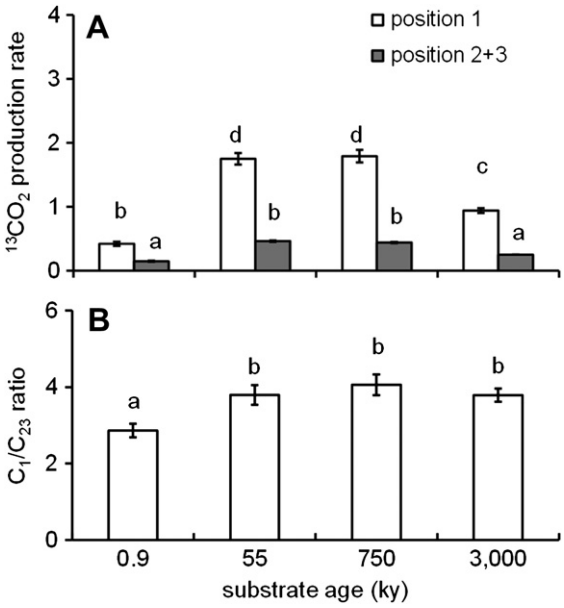

Fig. 6. $^{13}CO_2$ release rate from 1-^{13}C and 2,3-^{13}C pyruvate (A, nmol $^{13}CO_2$ g^{-1} h^{-1}) and $C_1/C_{2,3}$ ratio (B) for soil collected from the Substrate Age Gradient of Arizona. Rates and $C_1/C_{2,3}$ ratio are estimated from linear regression of $^{13}CO_2$ concentration between 0 and 120 min after pyruvate addition. Interaction between substrate age and C-position was significant ($P < 0.001$). Letters indicate significant differences (multiple means LSD test when ANOVA indicated significance).

pyruvate will also contain $C_{2,3}$, but most products that contain $C_{2,3}$ do not contain C_1. This conclusion is consistent with expectations from incubations with uniformly labeled substrate: labeled materials get incorporated in soil C pools with low turnover rates, and are released only slowly. We now know that certain C atoms in substrate molecules have a greater probability being incorporated in these pools than other C atoms. Carboxyl-C of glycine and alanine was also lost at a higher rate than the other C atoms (Kuzyakov, 1997; Näsholm et al., 2001). This is expected as alanine is and glycine may be broken down via pyruvate. Fisher and Kuzyakov (2010) suggested that the carboxyl group of acetate was similarly lost quickly, but differences in CO_2 production were only apparent at the highest acetate concentration. At lower concentrations, C_1 and C_2 of acetate were divided unevenly over the liquid and solid phase, but it was not known whether this was associated with decarboxylation to CO_2 or incorporation into microbial products, for example organic acids (Fisher and Kuzyakov, 2010). Similar to Fisher and Kuzyakov (2010) for acetate, we conclude that pyruvate uptake and processing is fast, with only small amounts adsorbed to soil mineral surfaces.

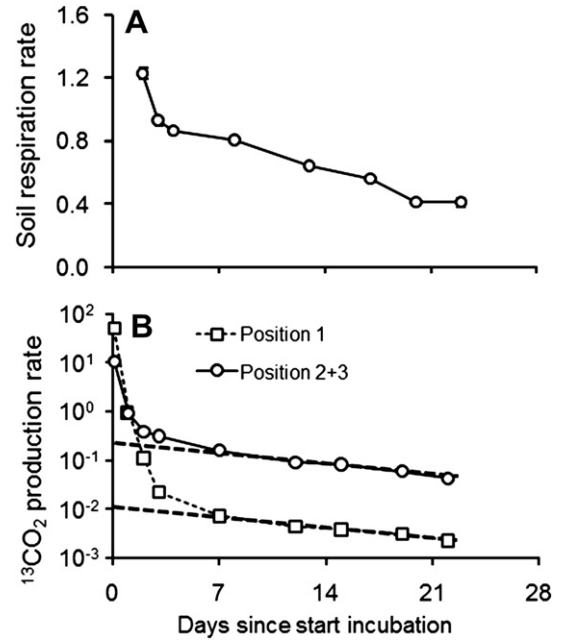

Fig. 7. Total soil respiration rate (A, μmol CO_2 g^{-1} soil d^{-1}) and $^{13}CO_2$ production rate from 1-^{13}C and 2,3-^{13}C-labeled pyruvate (B; nmol $^{13}CO_2$ g^{-1} soil h^{-1}, log scale) against incubation duration. Regression lines (dashed) for 1-^{13}C ($R^2 = 0.98$; $y = 0.015\ e^{-0.073x}$) and 2,3-^{13}C pyruvate ($R^2 = 0.98$; $y = 0.362\ e^{-0.084x}$) in (B) are based on the last two weeks of measurements.

Parallel incubation of pairs of metabolic tracer isotopologues is an essential element of this method. Mineral surfaces and organic matter may adsorb pyruvate to a variable degree in different soils, and pyruvate uptake by microbial cells may be influenced by environmental factors or substrate availability. Sorption and reduced uptake will decrease the absolute amount of $^{13}CO_2$ that is released from this molecule. However, these processes will be the same for both isotopologues of pyruvate, and therefore their ratio will not be affected. This ratio is used for inferring C flux patterns.

4.2. Interpretation of changes in $C_1/C_{2,3}$ ratio

Differences in $C_1/C_{2,3}$ ratio were evident within 10–20 min after pyruvate addition (Fig. 2), making this a potentially rapid method to determine the physiological condition of the soil microbial community. The $C_1/C_{2,3}$ ratio increased after low O_2 conditions were applied, decreased in the presence of glucose, pine and legume litter, and was lower for soil with a high C:N ratio. We interpret changes in this ratio as an indication of a changed C flux pattern through the microbial metabolic network, specifically altered activity of the glycolysis relative to the Krebs cycle. This qualitative interpretation is supported by our results in the following ways.

First, the observed increase in $C_1/C_{2,3}$ ratio in response to anaerobic conditions (Fig. 4B) suggests a decrease in Krebs cycle activity. Under anaerobic conditions, fermentation is stimulated while Krebs cycle activity is strongly inhibited (Chen et al., 2009). The presence of large quantities of alternative electron acceptors may alter this response. Under low O_2, an increased production of fermentation byproducts such as lactate, ethanol, acetate and many other compounds is expected (Chen et al., 2009; Hua and Shimizu, 1999; Zhu et al., 2006), so it is likely that more of the $C_{2,3}$ from pyruvate ends up in fermentation products that are secreted into the soil environment.

Second, we found that $^{13}CO_2$ production from pyruvate was strongly reduced in the presence of succinate, while total respiration rate was enhanced relative to the control soil (Figs. 2 and 3). Succinate can enter directly in the Krebs cycle, and induce gluconeogenesis when glucose concentrations are low (Sauer and Eikmanns, 2005). Gluconeogenesis is the process whereby carbohydrates are produced from small molecular organic compounds and involves an 'inversion' of glycolysis (Nelson and Cox, 2008). Under these conditions, pyruvate entry into the Krebs cycle is blocked (Holms, 1996), explaining the reduction of pyruvate utilization we observed.

Third, we observed a consistent pattern of low $C_1/C_{2,3}$ ratios with high glycolytic substrate availability (glucose, legume and pine litter and soil with high C:N ratio). We speculate that this was caused by an increased demand for energy and biosynthesis products associated with increased activity of the microbial community. This result differs from *in vitro* experiments with some

fast-growing microorganisms. Under glucose excess, *Escherichia coli* and *Bacillus subtilis* exhibit strong reductions of Krebs cycle activity (Dauner et al., 2001; Holms, 1996). These organisms maximize ATP production by stimulating substrate-level phosphorylation in glycolysis while lowering carbon use efficiency. A similar repression of Krebs activity is observed in human cancer cells (Grüning et al., 2010). The difference between *in vitro* results for fast-growing species and the soil microbial community may be caused by 1- a low proportion of fast-growing organisms in the soil microbial community in these short-term experiments, 2- much higher glucose concentrations under *in vitro* conditions.

4.3. Litter quality and soil substrate age

The $C_1/C_{2,3}$ ratio was significantly lower for soil amended with legume litter than with pine litter. This result shows that the metabolic tracer method may reveal differences in the response to litter quality. Longer-term experiments and experiments with a broader array of plant substrates are needed to see whether these observations can be generalized. The low $C_1/C_{2,3}$ ratio for the legume litter may be related to the high N content, increasing the demand for amino acids and thus Krebs cycle intermediates. Alternatively, it may be caused by the high content of lignin and resins in pine needles. Lignin and resins are ignored or broken down to small organic gluconeogenic compounds, such as glycolaldehyde, oxalate, succinate and acetate (Hammel et al., 1994; Ornston and Stanier, 1966), utilization of which reduces the entry of pyruvate into the Krebs cycle.

Young volcanic soils in tropical and semiarid climates exhibit strong N limitations (Coyle et al., 2009; Dijkstra et al., 2008; Hedin et al., 2003; Selmants and Hart, 2008). The relatively high C:N ratio and C availability in these young soils may explain the low $C_1/C_{2,3}$ ratio: an active Krebs cycle activity under high C availability results in a low $C_1/C_{2,3}$ ratio as found after glucose or litter addition. Although clay content (Table 1) and clay mineralogy likely change across the age gradient, changes in sorption to these minerals will not affect the ratio between the two isotopologues and therefore will not affect our conclusion.

4.4. Towards a quantitative metabolic flux analysis in soils

In the above analysis, we equate the $C_1/C_{2,3}$ ratio with the ratio of C fluxes through the decarboxylating steps of glycolysis and Krebs cycle. Although this qualitative interpretation is correct, a more quantitative interpretation of these observations requires clarification of additional aspects of soil microbial metabolic functioning.

1. The $C_1/C_{2,3}$ ratio under high glycolytic substrate availability can be affected by altered substrate utilization. For example, Schilling et al. (2007) demonstrated that more pyruvate entered the Krebs cycle when glucose was the only substrate compared to a situation where glucose, succinate and glutamate were utilized simultaneously. Therefore a change in substrate utilization after glucose addition may decrease the $C_1/C_{2,3}$ ratio when pyruvate is used as a metabolic tracer, in addition to the altered Krebs cycle activity. For a quantitative analysis of soil C metabolism, a more thorough understanding of substrate utilization is required.
2. The demand for Krebs cycle intermediates increases when biosynthesis increases. These intermediates need to be replenished in order to maintain Krebs cycle activity. This replenishment occurs via anaplerotic processes of phosphoenolpyruvate and pyruvate carboxylase, or from other C sources, for example organic acids or acetate if they are present. Pyruvate carboxylase enables entry of C_1 into the Krebs cycle, but the degree to which this occurs in soils is unknown. However, a strong pyruvate carboxylase activity implies that the $C_1/C_{2,3}$ ratio underestimates the shifts in relative activities of glycolysis to Krebs cycle. The C flux partitioning between pyruvate carboxylase and pyruvate dehydrogenase needs to be estimated using additional metabolic tracers in order to arrive at a quantitative model of C cycling processes.

More studies of C flux through soil metabolic processes are clearly needed. One approach we advocate is the use of multiple metabolic tracers. Each tracer will reflect different aspects of the overall metabolic system in soils, and in combination may reveal many more details of regulation of C fluxes through the soil microbial community. The results of this study hold promise that metabolic tracers can be used as tools to characterize the metabolic network in soil microbial communities. The parallel position-specific metabolic tracer labeling can be used in lab incubations (this study) and undisturbed soils in the field (Blankinship and Dijkstra, unpublished results). These measurements are fast, making it more likely that the real physiological processes are characterized, especially since the experimental conditions can be kept close to what is expected for real soil ecosystems.

Acknowledgements

This paper was inspired by recent studies of C isotope fractionation during respiration in plants (Priault et al., 2009) and a stimulating review by Hobbie and Werner (2004). We also thank two anonymous reviewers for their thoughtful and detailed comments. This project is financially supported by grants from the US Department of Agriculture National Research Initiative (NRI 2005-35107-16191) from the USDA National Institute of Food and Agriculture, National Science Foundation Major Research Instrumentation Program (DBI-0723250), and the Northern Arizona University Technology and Research Initiative Fund (Environmental Research, Development, and Education for the New Economy).

References

Allen, A.S., Schlesinger, W.H., 2004. Nutrient limitations to soil microbial biomass and activity in loblolly pine forests. Soil Biology & Biochemistry 36, 581–589.

Bago, B., Pfeffer, P.E., Douds, D.D., Brouillette, J., Bécard, G., Shacher-Hill, Y., 1999. Carbon metabolism in spores of the arbuscular mycorrhizal fungus *Glomus intraradices* as revealed by nuclear magnetic resonance spectroscopy. Plant Physiology 121, 263–271.

Chen, Z., Liu, H.-J., Zhang, J.-A., Liu, D.-H., 2009. Cell physiology and metabolic flux response of *Klebsiella pneumonia* to aerobic conditions. Process Biochemistry 44, 862–868.

Coyle, J.S., Dijkstra, P., Doucett, R.R., Schwartz, E., Hart, S.C., Hungate, B.A., 2009. Relationships between C and N availability, substrate age, and natural abundance ^{13}C and ^{15}N signatures of soil microbial biomass in a semiarid climate. Soil Biology & Biochemistry 41, 1605–1611.

Dauner, M., Storni, T., Sauer, U., 2001. *Bacillus subtilis* metabolism and energetics in carbon-limited and excess-carbon chemostat culture. Journal of Bacteriology 183, 7308–7317.

Dijkstra, P., Ishizu, A., Doucett, R.R., Hart, S.C., Schwartz, A., Menyailo, O., Hungate, B.A., 2006. ^{13}C and ^{15}N natural abundance of the soil microbial biomass. Soil Biology & Biochemistry 38, 3257–3266.

Dijkstra, P., LaViolette, C., Coyle, J.S., Doucett, R.R., Schwartz, E., Hart, S.C., Hungate, B.A., 2008. ^{15}N enrichment as an integrator of the effects of C and N on microbial metabolism and ecosystem function. Ecology Letters 11, 389–397.

Fisher, H., Kuzyakov, Y., 2010. Sorption, microbial uptake and decomposition of acetate in soil: transformations revealed by position-specific ^{14}C labeling. Soil Biology & Biochemistry 42, 186–192.

Grüning, N.-M., Lehrauch, H., Ralser, M., 2010. Regulatory crosstalk of the metabolic network. Trends in Biochemical Sciences 35, 220–227.

Haider, K., Martin, J.P., 1981. Decomposition in soil of specifically ^{14}C-labeled model and cornstalk lignins and coniferyl alcohol over two years as influenced by drying, rewetting, and additions of an available C substrate. Soil Biology & Biochemistry 13, 447–450.

Hammel, K.E., Mozuch, M.D., Jensen, K.A., Kersten, P.J., 1994. H_2O_2 recycling during oxidation of the arylglycerol β-aryl ether lignin structure by lignin peroxidase and glyoxal oxidase. Biochemistry 33, 13349–13354.
Hart, S.C., Nason, G.E., Myrold, D.D., 1994. Dynamics of gross nitrogen transformations in an old-growth forest: the carbon connection. Ecology 75, 880–891.
Haubensak, K.A., Hart, S.C., Stark, J.M., 2002. Influences of chloroform exposure time and soil water content on C and N release in forest soils. Soil Biology & Biochemistry 34, 1549–1562.
Hedin, L.O., Vitousek, P.M., Matson, P.A., 2003. Nutrient losses over four million years of tropical forest development. Ecology 84, 2231–2255.
Hobbie, S.E., Vitousek, P.M., 2000. Nutrient limitation of decomposition in Hawaiian forests. Ecology 81, 1867–1877.
Hobbie, E.A., Werner, R.A., 2004. Intramolecular, compound-specific, and bulk carbon isotope patterns in C_3 and C_4 plants: a review and synthesis. New Phytologist 161, 371–385.
Holms, H., 1996. Flux analysis and control of the central metabolic pathways in *Escherichia coli*. FEMS Microbiology Reviews 19, 85–116.
Hua, Q., Shimizu, K., 1999. Effect of dissolved oxygen concentration on the intracellular flux distribution for pyruvate fermentation. Journal of Biotechnology 68, 135–147.
Kiefer, P., Heinzle, E., Zelder, O., Wittmann, C., 2004. Comparative metabolic flux analysis of lysine-producing *Corynebacterium glutamicum* cultured on glucose or fructose. Applied and Environmental Microbiology 70, 229–239.
Koletzko, B., Demmelmair, H., Hartl, W., Kindermann, A., Koletzko, S., Sauerwald, T., Szitanyi, P., 1998. The use of stable isotope techniques for nutritional and metabolic research in paediatrics. Early Human Development 53 (Suppl.), S77–S97.
Kruger, N.J., Ratcliffe, R.G., 2009. Insights into plant metabolic networks from steady-state metabolic flux analysis. Biochimie 91, 697–702.
Kuzyakov, 1997. Abbau von mit ^{14}C spezifisch markierten aminosäuren im boden und decarboxylierung als einer der natürlichen neutralisationsmechanismen. Archiv für Acker- und Pflanzenbau und Bodenkunde 41, 335–343.
Näsholm, T., Huss-Danell, K., Högberg, P., 2001. Uptake of glycine by field grown wheat. New Phytologist 150, 59–63.
Nelson, D.L., Cox, M.M., 2008. Lehninger – Principles of Biochemistry, fifth ed. WH Freeman and Company, New York.
Ornston, L.N., Stanier, R.Y., 1966. The conversion of catechol and protocatechuate to β-ketoadipate by *Pseudomonas putida*. The Journal of Biological Chemistry 241, 3776–3786.
Priault, P., Wegener, F., Werner, C., 2009. Pronounced differences in diurnal variation of carbon isotope composition of leaf respired CO_2 among functional groups. New Phytologist 181, 400–412.
Sauer, U., Eikmanns, B.J., 2005. The PEP-pyruvate-oxaloacetate node as the switch point for carbon flux distribution in bacteria. FEMS Microbiology Reviews 29, 765–794.
Schilling, O., Frick, O., Herzberg, C., Ehrenreich, A., Heinzle, E., Wittmann, C., Stülke, J., 2007. Transcriptional and metabolic responses of *Bacillus subtilis* to the availability of organic acids: transcription regulation is important but not sufficient to account for metabolic adaptation. Applied and Environmental Microbiology 73, 499–507.
Schlesinger, W., Andrews, J., 2000. Soil respiration and the global carbon cycle. Biogeochemistry 48, 7–20.
Selmants, P.C., Hart, S.C., 2008. Substrate age and tree islands influence carbon and nitrogen dynamics across a retrogressive semiarid chronosequence. Global Biogeochemical Cycles 22. doi:10.1029/2007/GB003062 2008.
Vitousek, P.M., Howarth, R.W., 1991. Nitrogen limitation on land and in the sea: how can it occur? Biogeochemistry 13, 87–115.
Vo, T.D., Greenberg, H.J., Palsson, B.O., 2004. Reconstruction and functional characterization of the human mitochondrial metabolic network based on proteomic and biochemical data. Journal Biological Chemistry 279, 39532–39540.
Zhu, J., Shalel-Levanon, S., Bennett, G., San, K.-Y., 2006. Effect of the global redox sensing/regulation networks on *Escherichia coli* and metabolic flux distribution based on C-13 labeling experiments. Metabolic Engineering 8, 619–627.